Controlled Doping of Carbon Nanotubes with Metallocenes for Application in Hybrid Carbon Nanotube/Si Solar Cells

ARTICLE *in* NANO LETTERS · APRIL 2014

Impact Factor: 13.59 · DOI: 10.1021/nl500894h · Source: PubMed

13 AUTHORS, INCLUDING:

Xiaokai Li
Yale University
15 PUBLICATIONS **316** CITATIONS
SEE PROFILE

Louise M Guard
Yale University
16 PUBLICATIONS **124** CITATIONS
SEE PROFILE

Jianguo Wu
Yale University
23 PUBLICATIONS **441** CITATIONS
SEE PROFILE

Sohrab Ismail-Beigi
Yale University
139 PUBLICATIONS **2,671** CITATIONS
SEE PROFILE

NANO LETTERS

Letter

pubs.acs.org/NanoLett

Controlled Doping of Carbon Nanotubes with Metallocenes for Application in Hybrid Carbon Nanotube/Si Solar Cells

Xiaokai Li,[†] Louise M. Guard,[‡] Jie Jiang,[§] Kelsey Sakimoto,[†] Jing-Shun Huang,[†] Jianguo Wu,[‡] Jinyang Li,[†] Lianqing Yu,[†] Ravi Pokhrel,[‡] Gary W. Brudvig,[‡] Sohrab Ismail-Beigi,[§] Nilay Hazari,*[,‡] and André D. Taylor*[,†]

[†]Department of Chemical and Environmental Engineering and [‡]Department of Chemistry, Yale University, New Haven, Connecticut 06511, United States

[§]Department of Applied Physics, Yale University, New Haven, Connecticut 06520, United States

Supporting Information

ABSTRACT: There is considerable interest in the controlled p-type and n-type doping of carbon nanotubes (CNT) for use in a range of important electronics applications, including the development of hybrid CNT/silicon (Si) photovoltaic devices. Here, we demonstrate that easy to handle metallocenes and related complexes can be used to both p-type and n-type dope single-walled carbon nanotube (SWNT) thin films, using a simple spin coating process. We report n-SWNT/p-Si photovoltaic devices that are >450 times more efficient than the best solar cells of this type currently reported and show that the performance of both our n-SWNT/p-Si and p-SWNT/n-Si devices is related to the doping level of the SWNT. Furthermore, we establish that the electronic structure of the metallocene or related molecule can be correlated to the doping level of the SWNT, which may provide the foundation for controlled doping of SWNT thin films in the future.

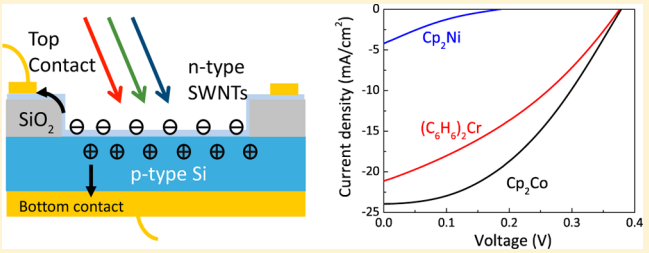

KEYWORDS: *Metallocenes, carbon nanotubes, doping, photovoltaic devices, density functional theory*

Single-walled carbon nanotubes (SWNTs) possess fascinating electrical properties and offer new entries into a wide range of novel electronics applications, including transistors,[1−3] solar cells,[4−7] displays,[8] and supercapacitors.[9] For practical applications, it is critical to obtain both p-type and n-type SWNTs, as p−n junctions are a fundamental component of a large number of conventional microelectronics devices.[10] At the moment, for both n-type and p-type exohedral doping, relatively few physical or electronic properties of the dopants, which correlate to the doping level of SWNTs, have been identified.[11] In general, this makes it difficult to predict doping levels. The most common method for exohedral doping of SWNTs is through charge transfer from noncovalently bound electron withdrawing or donating molecules. Although p-type SWNTs are naturally obtained in ambient conditions, due to the absorption of oxygen,[12] heavier and better controlled p-type doping is observed upon absorption of electron withdrawing molecules such as HNO_3,[13] $SOCl_2$,[14] tetrafluorotetracyano-p-quinodimethane,[15] gold salts,[16] and bis(trifluoromethanesulfonyl)imide.[17] Similarly, there are a range of electron donating molecules such as β-nicotinamide adenine dinucleotide (NADH),[18] viologens,[19] and amine-containing polymers like polyethylenimine (PEI),[20,21] which can n-type dope SWNTs. However, in general these stable molecules do not give high n-doping levels and the resulting n-type SWNTs have limited value in devices. Instead, significantly more reactive and sensitive compounds such as hydrazine[20] or potassium[22] are required to achieve a high level of n-type doping of SWNTs. Therefore, there is a need to find less reactive and more stable small molecules that can effectively generate n-type SWNTs for use in devices.

An interesting application for doped SWNTs is in hybrid SWNT/silicon (Si) photovoltaics. Recently a number of efficient p-type carbon nanotubes (CNT)/Si devices have been reported,[6,7,14,23−27] where the p-type behavior of the CNTs is obtained by doping with HNO_3,[7,24] $SOCl_2$,[14] or $HAuCl_4$.[6,7] The main advantage of these hybrid solar cells is that the intrinsically high photovoltaic efficiency of Si can be realized in a cost-effective manner owing to the low-temperature solution processability inherent to the fabrication of SWNT/Si junctions. Despite the progress on p-SWNT/n-Si solar cells, there are relatively few examples of n-SWNT/p-Si solar cells due to the difficulty in obtaining highly transparent n-type SWNTs with a suitable doping level. To date, the most efficient n-SWNT/p-Si photovoltaic device was reported by Li and co-workers,[21] who used PEI to n-type dope the SWNTs and obtained a low power conversion efficiency of 0.01% due to a very low short circuit current.

Received: March 9, 2014
Revised: April 23, 2014

   dx.doi.org/10.1021/nl500894h | *Nano Lett.* XXXX, XXX, XXX−XXX

Metallocenes and their derivatives are widely studied organometallic compounds that have numerous industrial applications.[28] They are relatively stable, easy to handle, and both the steric and electronic properties of the compounds are readily tunable. Previously, it has been shown that high-temperature thermal encapsulation of metallocenes in SWNTs can perturb the structural and electronic properties of the SWNTs, and this has been supported by theoretical calculations.[29−31] However, at this stage SWNT/metallocene composites have not been used in devices and it is unclear if the electronic properties of SWNT thin films can be modified by simply depositing metallocenes from solution. Here, we generate both p-type and n-type doped SWNT thin films, through a straightforward process involving spin coating different metallocenes and related molecules onto SWNT thin films. We have used the sheet resistance, electronic performance of hybrid SWNT/Si photovoltaic devices, and UV−vis spectroscopy to study the SWNT/metallocene composites. In particular, we report n-SWNT/p-Si solar cells that are >450 times more efficient than the best cells of this type reported to date. In addition, we demonstrate that the electronic structure of the metallocene or related molecule is correlated to the doping level of the SWNT, which may provide the foundation for the controlled doping of SWNT thin films in the future.

Several studies have suggested that the encapsulation of cobaltocene (Cp_2Co) into SWNTs results in charge transfer from the electron rich metal complex to the SWNT.[30,31] Unfortunately, the physical process of encapsulation is not straightforward,[31] and the level of doping in these metallocene/SWNT composites has not been determined. Given that metallocenes are easy to handle compared to powerful n-type dopants such as potassium or neat hydrazine, we were interested in finding a simple solution-based processing method to generate n-type SWNT thin films for use in hybrid n-SWNT/p-Si solar cells, where n-type doping of the SWNTs was achieved using an electron rich late transition metal metallocene. To prepare high quality SWNT thin films, we utilized a "superacid sliding coating method", which we had previously developed.[7] This process involves the use of chlorosulfonic acid, which strongly p-dopes CNTs due to the in situ generation of sulfuric acid.[32] In addition, CNTs naturally exhibit p-type behavior in air, which withdraws electrons from the CNTs.[12] As a result, it was not surprising that devices of as-transferred SWNT thin films on p-Si exhibit resistor behavior with no photocurrent rectification behavior under 1 sun illumination (Supporting Information Figure S1; for the SWNT/Si device fabrication method, see Methods).

In order to prepare samples for this n-type doping study, we placed our as made SWNT/p-Si devices in ultrahigh vacuum (10^{-7} mbar) at room temperature for 48 h to minimize the effect of oxygen and residual sulfuric acid from the treatment of the SWNTs with chlorosulfonic acid. Following this procedure, the electron rich metallocenes Cp_2Co and nickelocene (Cp_2Ni) and the closely related complex bis(benzene)chromium ($(C_6H_6)_2Cr$) were spin coated at room temperature onto the SWNT/p-Si devices. To further minimize the effect of oxygen, all doping experiments were performed inside a nitrogen-filled glovebox unless otherwise specified. Figure 1 shows the structures of the metallocenes and related complexes used in this study, while Figure 2a illustrates the structure of our n-SWNT/p-Si solar cells and Figure 2b shows the current density−voltage ($J-V$) curve for representative SWNT/p-Si

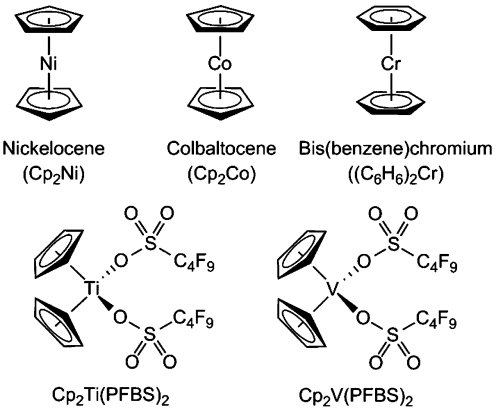

Figure 1. Structures of metallocenes and related complexes used in this study.

solar cells under 1 sun illumination (P_{input} = 100 mW/cm^2, AM 1.5 illumination) doped with electron rich metallocenes or related complexes. As a control, our metallocene-doped devices were compared to n-SWNT/p-Si solar cells in which hydrazine was used as the n-type dopant (Supporting Information Figure S2).

Our results clearly demonstrate that diode behavior occurs for all three metallocenes, suggesting that our simple spin coating procedure is sufficient for generating n-type doped SWNTs. Both Cp_2Co and $(C_6H_6)_2Cr$ doped devices give greater efficiency than hydrazine doped devices and the Cp_2Co doped devices are more stable (Supporting Information Figure S2). The highest power conversion is observed in Cp_2Co doped devices, whose extracted device parameters are as follows: the short circuit current (J_{sc}) is 23.9 mA/cm^2, the open circuit voltage (V_{oc}) is 0.379 V, and the fill factor (FF) is 0.422, which results in a power conversion efficiency (PCE) of 3.82%. To the best of our knowledge, this is over 350 times higher than the largest previously reported PCE for n-SWNT/p-Si solar cells,[21] whose performances suffer from high sheet resistance and low transparency in the SWNT films. The ideality factor of Cp_2Co doped devices extracted from the dark $J-V$ curve (Figure 2c) is 1.30, which is comparable to previous p-SWNT/n-Si solar cells,[24] indicating that good quality junctions are formed. The PCEs for Cp_2Ni and $(C_6H_6)_2Cr$ doped SWNT/p-Si devices are lower, 0.14% and 2.77%, respectively, with ideality factors of 1.41 observed in both cases. Detailed information on V_{oc}, J_{sc}, and FF are summarized in Table 1.

Currently, state-of-the-art p-SWNT/n-Si solar cells give a PCE of 8.52% with J_{sc} = 26.11 mA/cm^2, V_{oc} = 0.51 V, FF = 0.64 before light management (antireflective coating or scattering by nanoparticles).[7] A comparison of the performance of our best new n-SWNT/p-Si solar cells to these values indicates that the major differences are the lower V_{oc} and FF in n-SWNT/p-Si devices. The V_{oc} of SWNT/Si solar cells is highly correlated to the built-in potential, which is determined by the Fermi level of SWNTs with Si of fixed carrier concentration.[33] Therefore, we believe that the decrease in the V_{oc} is simply the result of less efficient n-type doping of the SWNTs compared to p-type doping. Low doping also results in less carrier density in SWNTs and thus high sheet resistance. As dissociated carriers need to travel through the SWNT emitter layer before being collected by the metal contacts, a high sheet resistance causes a high series resistance in solar devices and a lower FF.

dx.doi.org/10.1021/nl500894h | Nano Lett. XXXX, XXX, XXX−XXX

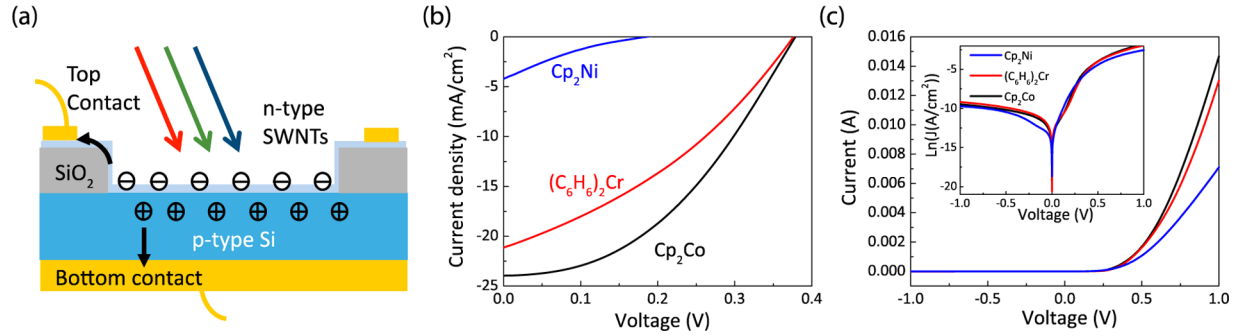

Figure 2. Performance of metallocene-doped SWNT/p-Si solar cells. (a) Schematic of n-SWNT/p-Si photovoltaic devices. (b) $J-V$ characteristics of Cp_2Ni (blue), $(C_6H_6)_2Cr$ (red), and Cp_2Co (black) doped n-SWNT/p-Si solar cells under 1 sun (AM1.5) illumination. (c) $I-V$ and ln$J-V$ characteristics of Cp_2Ni (blue), $(C_6H_6)_2Cr$ (red), and Cp_2Co (black) doped n-SWNT/p-Si solar cells in the dark.

Table 1. Summary of the Photovoltaic Characteristics of SWNT/Si Solar Cells Doped with Metallocenes and Related Complexes

doping type	doping complex	efficiency (%)	V_{oc} (V)	J_{sc} (mA/cm^2)	FF	ideality factor
n-type	Cp_2Ni	0.14	0.180	4.2	0.183	1.41
	$(C_6H_6)_2Cr$	2.77	0.376	21.1	0.348	1.41
	Cp_2Co	3.82	0.379	23.9	0.422	1.30
	Cp_2Co + current stimulation	4.62	0.426	24.2	0.449	1.40
p-type	$Cp_2Ti(PFBS)_2$	2.44	0.368	18.7	0.356	1.55
	$Cp_2V(PFBS)_2$	6.00	0.474	23.9	0.529	1.52

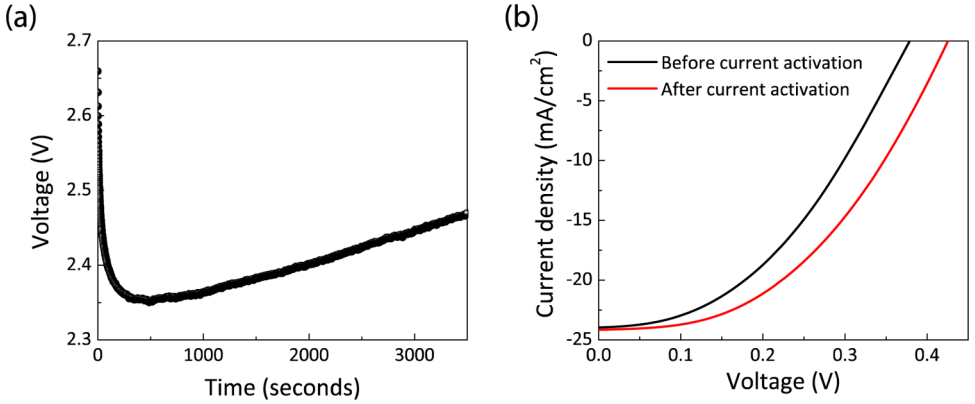

Figure 3. Current activation of SWNT/p-Si devices. (a) n-SWNT/p-Si response (voltage vs time) to 80 mA constant current stimulation. (b) $J-V$ characteristics of a Cp_2Co doped n-SWNT/p-Si solar cell before (black) and after (red) current activation under 1 sun (AM1.5) illumination.

Although our devices were placed under ultrahigh vacuum to remove oxygen, it is known that oxygen desorption from SWNTs is an extremely slow process, even under ultrahigh vacuum.[34] Furthermore, deoxygenated SWNTs can return to a p-type state by exposure to gas mixtures containing as little as 10^{-5} Torr of oxygen.[34] Therefore, we were concerned that our devices still contained residual oxygen, which would result in lower build in potentials and higher series resistance in our n-SWNT/p-Si devices. A different method for removing oxygen from SWNTs involves running constant current through the SNWT.[35] At certain voltages and currents, Poole-Frenkel conduction is the dominant pathway for electron transport.[36] In this regime, electrons jump over defects in the surface of CNTs due to high local electric fields and then continue along the CNT. Alternatively electrons can skip between molecules adsorbed onto a CNT and stimulate molecules to desorb. We tested whether we could desorb more oxygen from the SWNTs by applying a constant current through the anode and cathode of our SWNT/Si devices. Figure 3a shows the voltage versus time for Cp_2Co doped n-SWNT/p-Si solar cells with applied current of 80 mA. The changing voltage with time signals the gas desorption process. Figure 3b is the $J-V$ characteristic of a Cp_2Co doped n-SWNT/p-Si device before and after current stimulated oxygen desorption under 1 sun illumination. In agreement with our hypothesis, the V_{oc} improved more than 12% from 0.379 to 0.426 V; the J_{sc} improved slightly from 23.9 mA/cm^2 to 24.2 mA/cm^2, and the FF increased from 0.422 to 0.449. As a result, the PCE was enhanced by ∼21% to a new record of 4.62%, presumably due to increased n-type doping of the SWNT thin film. This result is consistent with previous reports that oxygen reabsorption takes place at very low levels of oxygen and that current stimulation is effective in removing oxygen from SWNT surfaces.[37] It also highlights the importance of oxygen removal in obtaining high performance n-SWNT/p-Si solar cells.

We were interested in exploring whether the photovoltaic performance of our n-SWNT/p-Si devices could be correlated to the electronic structure of the dopants. Previously, while

dx.doi.org/10.1021/nl500894h | Nano Lett. XXXX, XXX, XXX−XXX

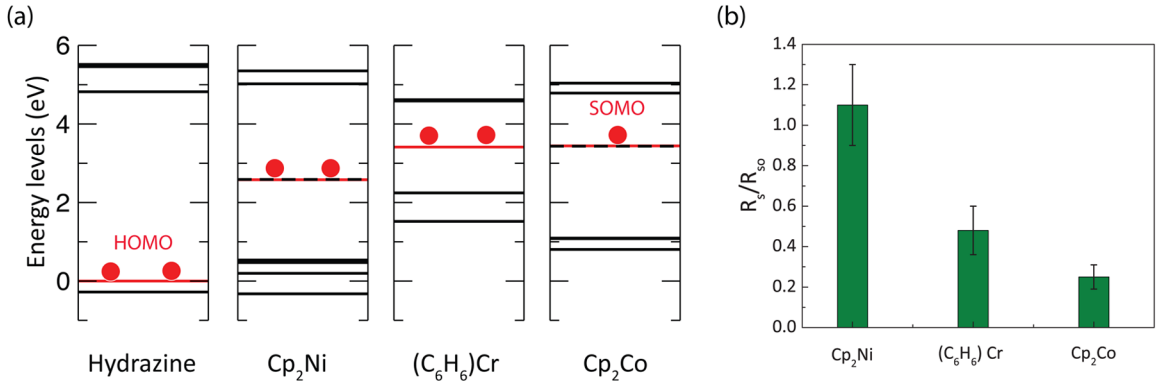

Figure 4. Energy levels of metallocenes and their effect on SWNT thin films. (a) DFT calculated energy levels of various n-type dopants. The red lines correspond to the highest energy levels that are occupied by electrons, which can provide n-type doping. The HOMO of hydrazine is used as a reference for the HOMO/SOMO of n-type dopants. (b) Normalized reduction in sheet resistance of SWNT thin films after treatment with various n-type dopants.

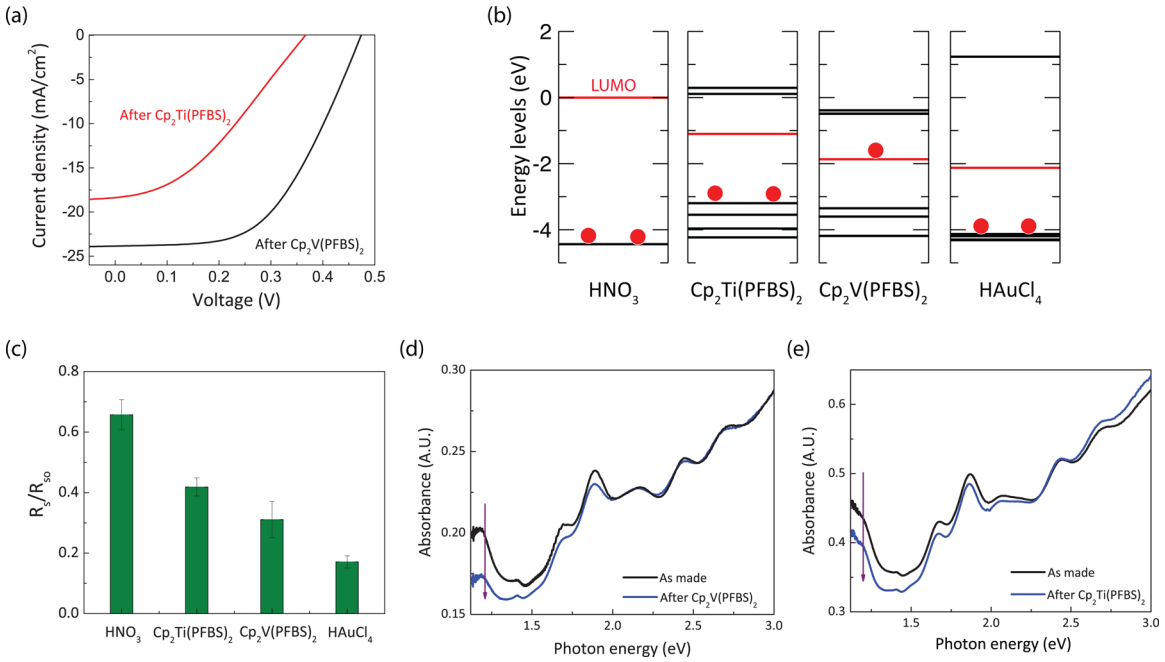

Figure 5. Energy levels of metallocene complexes and their effect on SWNT thin films and SWNT/n-Si devices. (a) $J-V$ characteristics of $Cp_2Ti(PFBS)_2$ (red) and $Cp_2V(PFBS)_2$ (black) doped p-SWNT/n-Si solar cells under 1 sun (AM1.5) illumination. (b) DFT calculated energy levels of various p-type dopants. The red lines correspond to the lowest energy orbitals that are fully or partially unoccupied and can provide p-type doping. The LUMO of HNO_3 is taken as the reference for the LUMO/SOMO of p-type dopants. (c) Normalized reduction in sheet resistance of SWNT thin films after treatment with various p-type dopants. Reduction of S_{22} absorption in SWNT after treatment with (d) $Cp_2V(PFBS)_2$ and (e) $Cp_2Ti(PFBS)_2$.

studying the encapsulation of small molecules in SWNTs, Takenobu et al. suggested that in some cases the carrier doping of SWNTs can be controlled by the ionization energy and electron affinity of the encapsulated material.[38] Although in our spin coating process it is unlikely that the metallocenes are encapsulated in the SWNTs, as the SWNTs were never opened, it is possible that a correlation also exists for adsorbed molecules. Density functional theory (DFT) calculations were performed to determine the energies of the molecular orbitals of Cp_2Co, $(C_6H_6)_2Cr$, and Cp_2Ni, as well as the previously known n-dopant hydrazine. (Please refer to the Supporting Information for the details of the DFT calculations. Supporting Information Figure S6 demonstrates the procedure for the DFT calculation of Cp_2Ni.) The DFT results are shown in Figure 4a. With hydrazine as a reference, the energy of the highest fully or partially filled orbitals (highest occupied molecular orbital (HOMO) or singly occupied molecular orbital (SOMO)) follows the order Cp_2Ni (2.58 eV) < $(C_6H_6)_2Cr$ (3.37 eV) < Cp_2Co (3.44 eV). There is clearly a strong correlation between the energies of the highest fully or partially filled orbitals and the efficiency of n-SWNT/p-Si photovoltaic performance, which we believe is related to the extent of n-doping. Sheet resistance measurements were performed to fully explore this relationship and investigate the level of n-doping that occurs with our dopants. Figure 4b shows the normalized sheet resistance of SWNT thin films on glass slides before and after doping with Cp_2Co, $(C_6H_6)_2Cr$ and Cp_2Ni. Doping with Cp_2Co gives the highest reduction in sheet resistance, 75%, while doping with $(C_6H_6)_2Cr$ gives a reduction of 52% and a slight increase of 10% is observed with Cp_2Ni. Given that the

dx.doi.org/10.1021/nl500894h | Nano Lett. XXXX, XXX, XXX−XXX

reduction in sheet resistance is caused by the injection of electrons into intrinsic SWNTs, which raises the Fermi level toward the conduction band (intrinsic SWNTs were obtained using a literature procedure),[20] a larger reduction in sheet resistance is consistent with higher n-type doping. This is consistent with our hypothesis that higher energies of the highest fully or partially filled orbitals of our dopants correspond to increased n-type doping and consequently higher n-SWNT/p-Si photovoltaic performance. Further evidence that metallocene doping results in n-type doping of SWNTs was obtained using Raman spectroscopy. A significant reduction in the G-band was observed when a Cp_2Co doped SWNT film was compared to an intrinsic SWNT film, as well as phonon softening by 3 cm^{-1} (Supporting Information Figure S3). Both of these results are indicative of n-type doping.[19,39]

To date there are relatively few classes of molecules that allow for the controlled doping of SWNTs, and there is no generic family of molecules that have been demonstrated to both p-type and n-type doping SWNTs. Given our results that electron rich late transition metal metallocenes could be used to n-type dope SWNTs, we hypothesized that electron deficient early transition metal metallocenes could be used for p-type doping SWNTs. Recently, Qiu et al. reported the preparation of a highly electron deficient titanocene with two perfluorobutanesulfonate ligands, $Cp_2Ti(PFBS)_2$ (Figure 1).[40] We synthesized this complex, along with its vanadium analogue $Cp_2V(PFBS)_2$, which was fully characterized as part of this work (see the Supporting Information for more details). To study the doping properties of these molecules in p-SWNT/n-Si devices, p-type doping from chlorosulfonic acid treatment and oxygen was removed using an HF and current stimulated oxygen removal process (Supporting Information Figure S4). Afterward, the SWNT is in a close to intrinsic state and the resulting SWNT/n-Si devices exhibit resistor behavior (Supporting Information Figure S4). The details about the combined HF and current stimulated oxygen removal process will be discussed in another publication. The SWNT/n-Si devices were then doped with $Cp_2Ti(PFBS)_2$ or $Cp_2V(PFBS)_2$ using a similar room-temperature spin coating method to that described for the late transition metal metallocenes. Figure 5a compares the $J-V$ characteristics of devices with $Cp_2Ti(PFBS)_2$ and $Cp_2V(PFBS)_2$. In both cases, significant photocurrent is generated and the best PCE of 6.00% is observed in $Cp_2V(PFBS)_2$ doped devices. Although this efficiency is lower than those reported for $HAuCl_4$ doped p-SWNT/n-Si devices,[6] it is nevertheless noteworthy that metallocenes can be used to generate both p-SWNT/n-Si devices and n-SWNT/p-Si devices. Furthermore, we propose that the higher V_{oc}, J_{sc}, FF, and PCE in $Cp_2V(PFBS)_2$ doped systems compared to $Cp_2Ti(PFBS)_2$ doped systems is indicative of increased p-type doping of SWNTs by $Cp_2V(PFBS)_2$.

To determine if there was a correlation between photovoltaic device performance and the electronic structure of p-type dopants, DFT calculations (Figure 5b) were performed on $Cp_2V(PFBS)_2$ and $Cp_2Ti(PFBS)_2$, as well as on the known p-type dopants HNO_3 and $HAuCl_4$. Our results suggest that there is a relationship between the energy of the lowest energy orbital of the dopant that can accept an electron from a SWNT (LUMO or SOMO of the dopant) and device performance. In the case of $Cp_2V(PFBS)_2$, the SOMO level is −1.867 eV, versus a HNO_3 reference, whereas for $Cp_2Ti(PFBS)_2$ the LUMO level is −1.101 eV. For $HAuCl_4$, which gives the best reported p-SWNT/n-Si devices, the LUMO level is −2.124 eV. We propose that the LUMO or SOMO level of the dopant affects photovoltaic performance because it is related to the level of p-type doping of the SWNT, as molecules with a lower energy orbital to accept an electron can withdraw more electrons from SWNTs and thus increase the carrier density of holes. Sheet resistance measurements were used to further study this correlation (Figure 5c). The largest reduction in sheet resistance is achieved in $HAuCl_4$ doped systems with a reduction of (82.9%), followed by $Cp_2V(PFBS)_2$ (68.9%), $Cp_2Ti(PFBS)_2$ (58.1%), and then HNO_3 (34.3%). All experiments were performed using the same concentration of the doping agent (2 mM) to ensure a valid comparison. Further direct evidence of fine controlling of p-doping from the metallocene complexes $Cp_2V(PFBS)_2$ and $Cp_2Ti(PFBS)$ is seen in the reduction of the S_{22} SWNT absorption with doping.[41] The magnitude of the reduction is highly correlated to the carrier density and reductions of 33 (Supporting Information Figure S5), 15, and 9% (Figure 5d,e), respectively, were observed for $HAuCl_4$, $Cp_2V(PFBS)_2$, and $Cp_2Ti(PFBS)_2$ doped SWNT thin films.

In conclusion, we have demonstrated that a family of molecules, metallocenes or related complexes, can be used to generate both n-type and p-type SWNT thin films through a simple spin-coating procedure. Furthermore, the n-type doping level of the SWNT films can be improved through a current stimulated oxygen removal process. We have used this procedure to obtain n-SWNT/p-Si solar cells that are >450 times more efficient than previous photovoltaic devices of this type. In a potentially important observation for the design of future molecules for the controlled doping of SWNTs, we have shown that the electronic structure of the metallocene or related molecule can be correlated to the doping level of the SWNTs. In the case of n-type doping, the energy of the highest partially or fully occupied orbital that can donate electrons to a SWNT is correlated to the doping level, whereas for p-type doping the energy of the highest partially or fully unoccupied orbital that can accept electrons from a SWNT is related to the doping level. Further work to understand exactly how metallocenes interact with the SWNT thin films and design more efficient and stable dopants for SWNTs is ongoing in our laboratory.

Methods. *SWNT/Si Device Fabrication.* A 500 nm thermal oxide covered n-type Si (100) wafer (1−10 Ω·cm) was patterned with Au (80 nm, top contact and etch mask)/Cr (5 nm, adhesion layer) by photolithography. A Si window (3 × 3 mm^2) was exposed through wet-etching of the oxide. The back contacts were fabricated using Al following a buffered oxide etch (BOE) for 1 min. The SWNT thin films were transferred onto patterned Si wafers by floating on water and then picked up by the wafers.

Doping SWNT Thin Films. For n-type doping studies, 5 mM solutions of Cp_2Ni, $(C_6H_6)_2Cr$, or Cp_2Co were prepared in acetonitrile, while for p-type doping studies 5 mM solutions of $Cp_2Ti(PFBS)_2$ or $Cp_2V(PFBS)_2$ were prepared in dichloromethane. Inside a glovebox, 50 μL of the doping solution was dropped onto the SWNT/Si window immediately before spin coating at 2000 rpm. For n-type doping, all SWNT/p-Si devices were pretreated in ultrahigh vacuum (10^{-7} mbar) at room temperature for 48 h, while for p-type doping, all SWNT/n-Si devices were first treated with HF and then subjected to current stimulated oxygen removal inside a glovebox. The HF and current stimulated oxygen removal steps removes the effects of

dx.doi.org/10.1021/nl500894h | Nano Lett. XXXX, XXX, XXX−XXX

chlorosulfonic acid and oxygen from our SWNT/n-Si devices, the mechanism of which will be reported in the future.

Current Stimulated Gas Desorption Process. We applied various currents (ranging from 20 to 80 mA) between the cathode and the anode of SWNT/Si devices for a period of time (1 min to 4 h) and measured the desorption of gases via the change of voltage over time.

Sheet Resistance Study. Sheet-resistance measurements were performed using a Signatone four-point probe with 10 mil radius contacts and 40 mil spacing. A Keithley Model 2400 SourceMeter was used to apply current and measure the resulting potential drop. The voltage drop was measured with applied currents and converted to a sheet resistance using the approximation $[\pi/\ln 2]$*V/I $\cong$ 4.53*V/I. SWNT thin films for the sheet resistance study were fabricated using a spray coating method. The SWNTs (2 mg) were added to 30 mL of 1,2-dichloroethane (Sigma-Aldrich) followed by sonication for 6 h. The solution was centrifuged at 8000 rpm for 10 min. The supernatant of the resulting solution was sprayed onto a glass slide with a nitrogen gas brush pistol. The SWNT films were then heat treated to 300 °C under vacuum (10^{-7} mbar) to exclude any solvent effects. To create intrinsic SWNT films, the samples were immersed in a 4 M hydrazine solution (ethanol) under nitrogen and then exposed to air for 5 min.[20]

■ ASSOCIATED CONTENT

Supporting Information

SWNT thin film fabrication methods, procedures for DFT calculations of metallocenes and related complexes, and details of the synthesis and characterization of $Cp_2Ti(PFBS)_2$ and $Cp_2V(PFBS)_2$. This material is available free of charge via the Internet at http://pubs.acs.org.

■ AUTHOR INFORMATION

Corresponding Authors

*E-mail: (N.H.) nilay.hazari@yale.edu.
*E-mail: (A.D.T.) andre.taylor@yale.edu.

Author Contributions

The manuscript was written through contributions of all authors. All authors have given approval to the final version of the manuscript.

Notes

The authors declare no competing financial interest.

■ ACKNOWLEDGMENTS

X.L. and A.D.T. gratefully acknowledge the Sabotka Research Fund, Teracon Corp., and the National Science Foundation NSF-CBET-0954985 CAREER Award for partial support of this work. A.D.T., S.I.-B., J.J., and J.-S.H. acknowledge funding from the NSF via Grant SOLAR DMR 0934520. Primary support for the theoretical work was provided by the NSF via Grant SOLAR DMR 0934520. Computational facilities were supported by NSF Grant CNS 08-21132 and by the facilities and staff of the Yale University Faculty of Arts and Sciences High Performance Computing Center. Additional computations were carried out via the NSF TeraGrid and XSEDE resources through Grant TG-MCA08X007. A.D.T., N.H., L.G., and J.L. acknowledge collaborative funding from the Yale Climate and Energy Institute. Facilities use was supported by YINQE and NSF MRSEC DMR 1119826 (CRISP). We thank Dr. Michael Takase for assistance with X-ray crystallography.

■ REFERENCES

(1) Wang, C.; Hwang, D.; Yu, Z. B.; Takei, K.; Park, J.; Chen, T.; Ma, B. W.; Javey, A. *Nat. Mater.* **2013**, *12*, 899−904.
(2) Shulaker, M. M.; Hills, G.; Patil, N.; Wei, H.; Chen, H. Y.; PhilipWong, H. S.; Mitra, S. *Nature* **2013**, *501*, 526−530.
(3) Kauffman, D. R.; Star, A. *Angew. Chem., Int. Ed.* **2008**, *47*, 6550−6570.
(4) Jain, R. M.; Howden, R.; Tvrdy, K.; Shimizu, S.; Hilmer, A. J.; McNicholas, T. P.; Gleason, K. K.; Strano, M. S. *Adv. Mater.* **2012**, *24*, 4436−4439.
(5) Ramuz, M. P.; Vosgueritchian, M.; Wei, P.; Wang, C. G.; Gao, Y. L.; Wu, Y. P.; Chen, Y. S.; Bao, Z. N. *ACS Nano* **2012**, *6*, 10384−10395.
(6) Jung, Y.; Li, X.; Rajan, N. K.; Taylor, A. D.; Reed, M. A. *Nano Lett.* **2012**, *13*, 95−99.
(7) Li, X.; Jung, Y.; Sakimoto, K.; Goh, T. H.; Reed, M. A.; Taylor, A. D. *Energy Environ. Sci.* **2013**, *6*, 879−887.
(8) Wang, S.; Zeng, Q. S.; Yang, L. J.; Zhang, Z. Y.; Wang, Z. X.; Pei, T. A.; Ding, L.; Liang, X. L.; Gao, M.; Li, Y.; Peng, L. M. *Nano Lett.* **2011**, *11*, 23−29.
(9) Yang, Z. B.; Deng, J.; Chen, X. L.; Ren, J.; Peng, H. S. *Angew. Chem., Int. Ed.* **2013**, *52*, 13453−13457.
(10) Javey, A.; Kong, J. *Carbon Nanotube Electronics*; Springer: New York, 2009.
(11) Hu, L.; Hecht, D. S.; Grüner, G. *Chem. Rev.* **2010**, *110*, 5790−5844.
(12) Collins, P. G.; Bradley, K.; Ishigami, M.; Zettl, A. *Science* **2000**, *287*, 1801−1804.
(13) Dan, B.; Irvin, G. C.; Pasquali, M. *ACS Nano* **2009**, *3*, 835−843.
(14) Li, Z. R.; Kunets, V. P.; Saini, V.; Xu, Y.; Dervishi, E.; Salamo, G. J.; Biris, A. R.; Biris, A. S. *ACS Nano* **2009**, *3*, 1407−1414.
(15) Takenobu, T.; Kanbara, T.; Akima, N.; Takahashi, T.; Shiraishi, M.; Tsukagoshi, K.; Kataura, H.; Aoyagi, Y.; Iwasa, Y. *Adv. Mater.* **2005**, *17*, 2430−2434.
(16) Li, X.; Gittleson, F.; Carmo, M.; Sekol, R. C.; Taylor, A. D. *ACS Nano* **2012**, *6*, 1347−1356.
(17) Kim, S. M.; Jo, Y. W.; Kim, K. K.; Duong, D. L.; Shin, H. J.; Han, J. H.; Choi, J. Y.; Kong, J.; Lee, Y. H. *ACS Nano* **2010**, *4*, 6998−7004.
(18) Kang, B. R.; Yu, W. J.; Kim, K. K.; Park, H. K.; Kim, S. M.; Park, Y.; Kim, G.; Shin, H. J.; Kim, U. J.; Lee, E. H.; Choi, J. Y.; Lee, Y. H. *Adv. Funct. Mater.* **2009**, *19*, 2553−2559.
(19) Kim, S. M.; Jang, J. H.; Kim, K. K.; Park, H. K.; Bae, J. J.; Yu, W. J.; Lee, I. H.; Kim, G.; Loc, D. D.; Kim, U. J.; Lee, E. H.; Shin, H. J.; Choi, J. Y.; Lee, Y. H. *J. Am. Chem. Soc.* **2009**, *131*, 327−331.
(20) Mistry, K. S.; Larsen, B. A.; Bergeson, J. D.; Barnes, T. M.; Teeter, G.; Engtrakul, C.; Blackburn, J. L. *ACS Nano* **2011**, *5*, 3714−3723.
(21) Li, Z. R.; Saini, V.; Dervishi, E.; Kunets, V. P.; Zhang, J. H.; Xu, Y.; Biris, A. R.; Salamo, G. J.; Biris, A. S. *Appl. Phys. Lett.* **2010**, *96*, 033110.
(22) Zhou, C. W.; Kong, J.; Yenilmez, E.; Dai, H. J. *Science* **2000**, *290*, 1552−1555.
(23) Cui, K. H.; Chiba, T.; Omiya, S.; Thurakitseree, T.; Zhao, P.; Fujii, S.; Kataura, H.; Einarsson, E.; Chiashi, S.; Maruyama, S. *J. Phys. Chem. Lett.* **2013**, *4*, 2571−2576.
(24) Jia, Y.; Cao, A. Y.; Bai, X.; Li, Z.; Zhang, L. H.; Guo, N.; Wei, J. Q.; Wang, K. L.; Zhu, H. W.; Wu, D. H.; Ajayan, P. M. *Nano Lett.* **2011**, *11*, 1901−1905.
(25) Shi, E. Z.; Zhang, L. H.; Li, Z.; Li, P. X.; Shang, Y. Y.; Jia, Y.; Wei, J. Q.; Wang, K. L.; Zhu, H. W.; Wu, D. H.; Zhang, S.; Cao, A. Y. *Sci. Rep.* **2012**, *2*, 885−889.
(26) Wei, J. Q.; Jia, Y.; Shu, Q. K.; Gu, Z. Y.; Wang, K. L.; Zhuang, D. M.; Zhang, G.; Wang, Z. C.; Luo, J. B.; Cao, A. Y.; Wu, D. H. *Nano Lett.* **2007**, *7*, 2317−2321.
(27) Li, X.; Jung, Y.; Huang, J.-S.; Goh, T.; Taylor, A. D. *Adv. Energy Mater.* **2014**, DOI: 10.1002/aenm.201400186.
(28) Long, N. J. *Metallocenes: An Introduction to Sandwich Complexes*; Wiley-Blackwell: Oxford, 1998.

(29) Sceats, E. L.; Green, J. C. *J. Chem. Phys.* **2006**, *125*, 154704.
(30) Lu, J.; Nagase, S.; Yu, D. P.; Ye, H. Q.; Han, R. S.; Gao, Z. X.; Zhang, S.; Peng, L. M. *Phys. Rev. Lett.* **2004**, *93*, 116804.
(31) Li, L. J.; Khlobystov, A. N.; Wiltshire, J. G.; Briggs, G. A. D.; Nicholas, R. J. *Nat. Mater.* **2005**, *4*, 481−485.
(32) Hecht, D. S.; Heintz, A. M.; Lee, R.; Hu, L. B.; Moore, B.; Cucksey, C.; Risser, S. *Nanotechnology* **2011**, *22*, 075201.
(33) Miao, X. C.; Tongay, S.; Petterson, M. K.; Berke, K.; Rinzler, A. G.; Appleton, B. R.; Hebard, A. F. *Nano Lett.* **2012**, *12*, 2745−2750.
(34) Bradley, K.; Jhi, S. H.; Collins, P. G.; Hone, J.; Cohen, M. L.; Louie, S. G.; Zettl, A. *Phys. Rev. Lett.* **2000**, *85*, 4361−4364.
(35) Salehi-Khojin, A.; Lin, K. Y.; Field, C. R.; Masel, R. I. *Science* **2010**, *329*, 1327−1330.
(36) Perello, D. J.; Yu, W. J.; Bae, D. J.; Chae, S. J.; Kim, M. J.; Lee, Y. H.; Yun, M. *J. Appl. Phys.* **2009**, *105*, 124309.
(37) Bai, X.; Wei, J. Q.; Jia, Y.; He, S. Q.; Sun, H. H.; Zhu, H. W.; Wang, K. L.; Wu, D. H. *Appl. Phys. Lett.* **2013**, *102*, 143105.
(38) Takenobu, T.; Takano, T.; Shiraishi, M.; Murakami, Y.; Ata, M.; Kataura, H.; Achiba, Y.; Iwasa, Y. *Nat. Mater.* **2003**, *2*, 683−688.
(39) Rao, A. M.; Richter, E.; Bandow, S.; Chase, B.; Eklund, P. C.; Williams, K. A.; Fang, S.; Subbaswamy, K. R.; Menon, M.; Thess, A.; Smalley, R. E.; Dresselhaus, G.; Dresselhaus, M. S. *Science* **1997**, *275*, 187−191.
(40) Qiu, R. H.; Zhang, G. P.; Ren, X. F.; Xu, X. H.; Yang, R. H.; Luo, S. L.; Yin, S. F. *J. Organomet. Chem.* **2010**, *695*, 1182−1188.
(41) Geng, H. Z.; Lee, D. S.; Kim, K. K.; Han, G. H.; Park, H. K.; Lee, Y. H. *Chem. Phys. Lett.* **2008**, *455*, 275−278.

dx.doi.org/10.1021/nl500894h | *Nano Lett.* XXXX, XXX, XXX−XXX